An Investigation on EEG-based Prognosis Prediction of Patients with Disorders of Consciousness

Jingcong Li (lijingcong@hotmail.com)

Biao Huang (huangbiao@m.scnu.edu.cn)

Jiahui Pan (panjiahui@m.scnu.edu.cn)

Fei Wang (fwang@scnu.edu.cn)[1]

School of Software, South China Normal University, Wanjin Lu, Shishan Town, Nanhai District, Foshan, 528225, Guangdong Province, China

Abstract

Prognostic assessment of patients with disorders of consciousness (DoC) remains one of the most challenging problems in contemporary medicine. The long treatment cycle and high costs of treatment for DoC patients are heavy burdens to the patients' families and our society. Moreover, the currently used diagnostic and prognosis methods are imprecise that effective technique for auxiliary diagnosis on DoC is of great interest. In this paper, we use deep network to investigate potential indicators of consciousness within brain signals of DoC patients. In the experiments, we study P300 and resting-state Electroencephalogram (rs-EEG) signals of 22 DoC patients to investigate neural correlation between brain signals and the improvement of consciousness. Synergistic integration of P300 and rs-EEG signals demonstrated superior predictive proficiency for cross-subject and cross-paradigm prognosis in DoC, achieving an accuracy rate of 81.1%. Our results indicate that hybrid P300 and rs-EEG can be used to predict the prognosis of patients with DoC, and provide new evidence for the neural correlate of EEG signals to altered states of consciousness. Our investigation is the first known to the literature to combine P300 and rs-EEG signals within a deep learning architecture for analyzing DoC. This novel approach leverages advanced neural network models to elucidate the complex neural patterns associated with DoC, setting a precedent for future research in the field.

Keywords: Disorders of consciousness (DoC); Prognosis; P300; rs-EEG; deep network; cross-subject; cross-paradigm

Introduction

Disorders of consciousness (DoC) are severe sequelae of brain injury characterized by deficits in consciousness and cognitive impairment, including coma, unresponsive wakefulness syndrome (UWS, also known as a vegetative state), minimally conscious state (MCS), and locked-in syndrome (LIS) (Monti, Laureys, & Owen, 2010). For example, patients with UWS do not have discrete localized motor control, cannot articulate the words they want to express, and cannot spontaneously open their eyes to complete verbal commands (Laureys et al., 2010; Johnson & Lazaridis, 2018). They may wake up, but they are unaware of themselves or their environment (Jennett & Plum, 1972). Patients with MCS are characterized by inconsistent but reproducible signs of consciousness through behavior. Furthermore, a feature that emerged in MCS was reliable and consistent functional interaction communication or demonstration of functional usage by two different objects (Giacino et al., 2002).

Electroencephalogram (EEG) is a commonly used diagnostic technique in clinical neuromedicine, and its convenience and wide availability have led to its rapid emergence in the field of assessment of DoC (Gantner et al., 2013; Fernández-Espejo & Owen, 2013). EEG provides a signal of a patient's brain function, allowing the diagnosis of a patient's state of consciousness through non-behavioral EEG signals. After severe brain injury, brain activity will change dramatically, and EEG signals between different patients have great individual differences. Therefore, it is extremely challenging to predict the prognosis of cross-subjects through EEG signals.

In recent years, with the vigorous development of brain-computer interface (BCI) technology, more and more experts and scholars try to apply BCI technology to the clinical detection of consciousness (Pan et al., 2020; Luauté, Morlet, & Mattout, 2015), and explore an objective methods to assess the patient's level of consciousness and prognosis. For example, Pan et al. demonstrated the great potential of P300-based BCIs to effectively detect residual consciousness in DoC patients (Pan, Wang, et al., 2023). P300 is the third positive wave of event-related potential (ERP). It is an endogenous component that is not affected by physical characteristics (shape, size, vision, hearing, etc.) and is closely related to human cognitive functions. Compared with the existing methods, the use of P300-BCI technology can judge the patient's consciousness level more conveniently and quickly without basing on the patient's behavior.

In addition, resting-state electroencephalogram (rs-EEG) monitoring technique has also been shown to be a potentially powerful tool that can help physicians and clinical staff to rapidly assess the state of consciousness and prognosis of patients with DoC (Sitt et al., 2014; Bai, Xia, & Li, 2017; Bai, Lin, & Ziemann, 2021; Rossi Sebastiano et al., 2021). Moreover, the acquisition of rs-EEG signals is very simple and convenient. It is only necessary to use the corresponding BCI equipment at the patient's bedside and collect the patient's data, which is cost-effective. Rs-EEG recordings represent spontaneous neural activity, which correlates with the basal state of the brain (Giacino et al., 2014; Stam et al., 2005). Therefore, appropriate features from rs-EEG may help to monitor brain conditions in DoC and better communicate with physicians and caregivers to improve

[1]Corresponding author

In L. K. Samuelson, S. L. Frank, M. Toneva, A. Mackey, & E. Hazeltine (Eds.), *Proceedings of the 46th Annual Conference of the Cognitive Science Society.*

Table 1: The basic information and CRS-R scores of 22 patients.

					CRS-R scores (subscores)	
Patient	**Age**	**Gender**	**Etiology**	**BCI paradigm**	**Before experiment**	**After 3 months**
P01	22	F	ABI	Number	6 (1-0-2-1-0-2)	6 (1-0-2-1-0-2)
P02	48	M	ABI	Number	7 (1-1-2-1-0-2)	18 (4-5-5-1-1-2)
P03	47	M	TBI	Number	4 (1-1-0-0-0-2)	6 (1-0-2-1-0-2)
P04	37	F	TBI	Number	3 (0-0-1-0-0-2)	23 (4-5-6-3-2-3)
P05	27	F	CVD	Number	6 (1-0-2-1-0-2)	10 (2-0-4-2-0-2)
P06	43	M	TBI	Number	5 (1-0-1-1-0-2)	6 (1-0-2-1-0-2)
P07	19	M	CVD	Number	5 (1-0-1-1-0-2)	6 (1-0-2-1-0-2)
P08	51	M	TBI	Audiovisual	9 (2-1-2-2-0-2)	9 (2-1-2-2-0-2)
P09	29	M	ABI	Audiovisual	4 (1-0-1-0-0-2)	4 (1-0-1-0-0-2)
P10	37	M	ABI	Audiovisual	5 (0-0-2-1-0-2)	5 (0-0-2-1-0-2)
P11	38	M	TBI	Audiovisual	7 (1-1-2-1-0-2)	7 (1-1-2-1-0-2)
P12	33	M	TBI	Audiovisual	7 (1-0-2-2-0-2)	7 (1-0-2-2-0-2)
P13	38	M	TBI	Number	10 (1-3-3-1-0-2)	19 (3-5-6-1-1-3)
P14	46	F	CVD	Number	8 (1-2-2-1-0-2)	9 (1-2-3-1-0-2)
P15	53	F	TBI	Number	8 (1-2-2-1-0-2)	8 (1-2-2-1-0-2)
P16	44	M	CVD	Number	9 (1-3-2-1-0-2)	20 (4-5-6-2-1-2)
P17	52	M	TBI	Number	9 (1-3-2-1-0-2)	18 (3-5-6-1-1-2)
P18	48	M	TBI	Audiovisual	12 (1-2-5-1-0-2)	16 (3-3-5-2-1-2)
P19	34	M	TBI	Audiovisual	9 (1-1-5-1-0-1)	15 (4-4-5-1-0-1)
P20	37	M	TBI	Audiovisual	9 (1-3-2-1-0-2)	19 (3-5-6-2-1-2)
P21	20	M	TBI	Audiovisual	7 (1-0-3-1-0-2)	7 (1-0-3-1-0-2)
P22	19	M	ABI	Audiovisual	8 (1-1-3-1-0-2)	8 (1-1-3-1-0-2)

Note: F: Female; M: Male; ABI: acquired brain injury; CVD: cerebrovascular disease; TBI: traumatic brain injury.

patient treatment options. The functional connectivity of EEG describes the dependence of different regions in the brain and plays an important role in neuroscience research. It has been used to study various brain diseases related to cognitive function and DoC.

In this study, we explore putative EEG biomarkers of consciousness in patients with DoC and endeavor to elucidate the associations between patients' EEG profiles and their prognostic outcomes. The main contributions of this paper are summarized as follows:

(1) A novel hybrid EEG method is proposed for prognosis prediction of DoC patients.

(2) The proposed method demonstrates robust performance across diverse subjects and experimental paradigms, indicating its broad applicability and reliability.

(3) In a cohort of 22 individuals with DoC, the proposed method attained a predictive accuracy of 81.1% in forecasting improvements in patients' CRS-R scores within a three-month horizon.

Methods

Participants

This study involved 22 patients with DoC (17 males and 5 females; 12 UWS patients and 10 MCS patients; mean age 37.36 $\pm$ 10.99 years; **Table 1**) from the General Hospital of Guangzhou Military Common of People's Liberation Army, China. Their clinical diagnosis was based on the CRS-R, which includes six subscales of auditory, visual, motor, oral motor, communication, and arousal functions. These diagnostic results were discovered after long-term observation by multiple professional clinical personnel. The diagnostic type (UWS/VS or MCS) of DoC patients was determined by the CRS-R score. The inclusion criteria included: (1) a diagnosis of UWS or MCS, with no detectable command-following behavior observed during the week of admission; (2) more than 1 month since brain injury; and (3) no history of impaired vision or hearing. This study was approved by the Ethics Committee of the General Hospital of Guangzhou Military Common and complied with the ethical Code of Ethics of the World Medical Association (Declaration of Helsinki). Each patient's legal representative provided written informed consent for the experiments and the publication of the patient's personal details in this study.

All patients underwent CRS-R assessment twice: one week before the start of the experiment and three months later. We used the CRS-R score to judge the level of consciousness. For each patient, two experienced physicians performed CRS-R assessments at least twice during each assessment period. Increasing CRS-R scores represent a trend toward increasing levels of awareness.

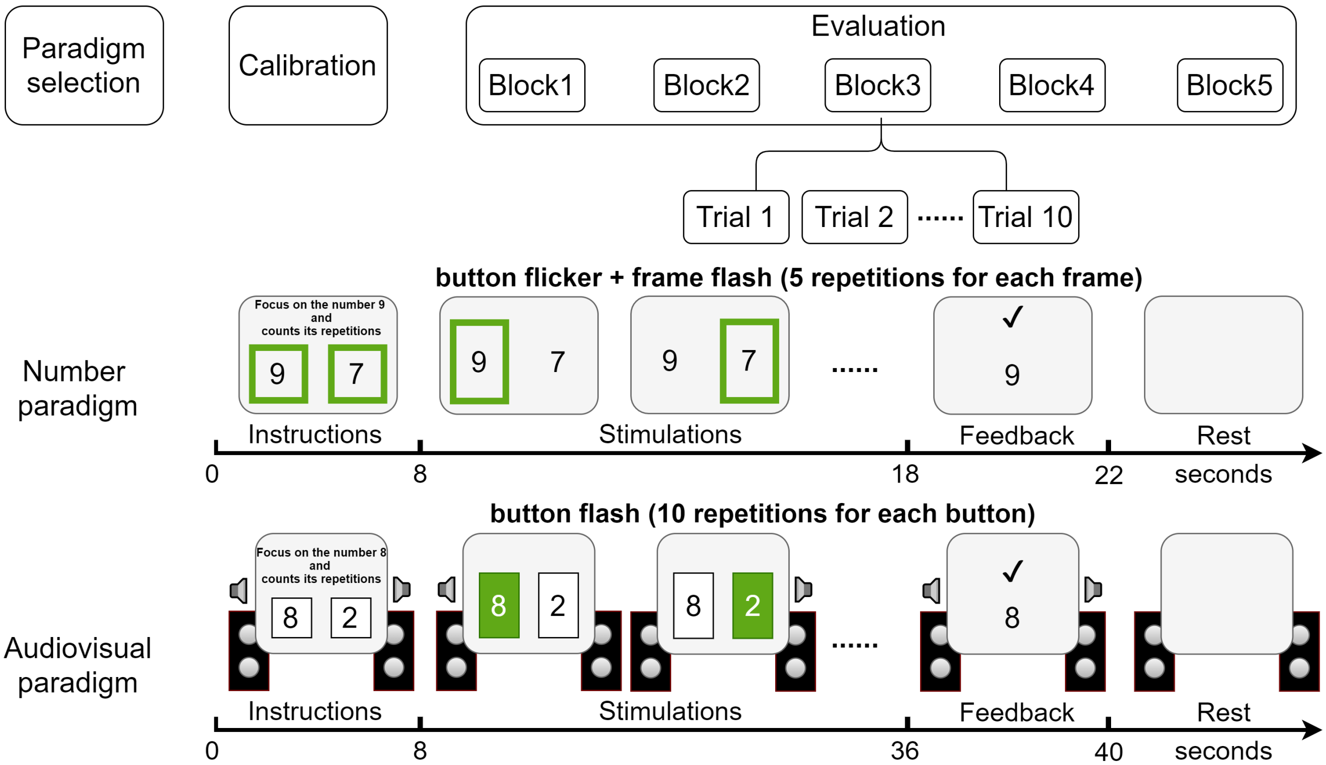

Figure 1: Illustration of the experimental design and procedure.

Procedure

Number Paradigm. As shown in **Figure 1**, in each experiment, two randomly selected Arabic numerals from 0 to 9 are presented. On each trial, one of the two photos was randomly selected as the target. Each trial began with an audiovisual description and two numbers, each embedded in a static frame. Instructions were displayed in Chinese characters for 8 seconds: "Focus on the target number and count the number of times the frame flashes." Following the instruction panel, a 10-second stimulation period began with two numbers simultaneously appearing on the screen. The two photos continued to flash at different frequencies (6.0 Hz and 7.5 Hz for the left and right numbers, respectively) to evoke the P300 associated with the left/right number.

Audiovisual Paradigm. For this paradigm, two buttons are located on the left and right sides of the GUI, each displaying two randomly selected Arabic numerals from 0 to 9. The buttons of the two numbers flash alternately, the color of the flashing button changes from green to black and the color of the corresponding number simultaneously changes from black to white. The corresponding number is simultaneously read from a speaker located on the same side of the monitor. In this way, subjects were presented with temporally, spatially, and semantically consistent audiovisual stimuli, each lasting 300 ms, to evoke a P300 response. The specific process is shown in **Figure 1**.

Preprocessing. For the entire BCI experimental process, we used NuAmps equipment (Compumedics Neuroscan, Inc. TX, USA.) to collect EEG data through 30 channels. EEG signals from all electrodes were referenced to the right mastoid and digitized at a sampling rate of 250 Hz. Electrode impedance was maintained below 5 KΩ. For each paradigm-related P300, the EEG signal was first filtered from 0.1 Hz to 10 Hz. For each flash of the frame surrounding the left image, we obtained a segment of the EEG signal from each channel (0-600 ms after the frame flash) and downsampled the segment at a fivefold rate. We concatenate the downsampled segments of the 10 channels (Fz, Cz, P7, P3, Pz, P4, P8, O1, Oz, and O2) to obtain the data vector for each flash. These were then averaged to provide a final correlated P300 feature vector for each trial. Through the above frequency band filtering and feature extraction methods, the influence of 50 Hz, electrocardiographic and myoelectrical artifacts of the AC power supply is removed. For each stimulus, EEG epochs for each channel were obtained from 50 ms before to 600 ms after stimulation after bandpass filtering (0.1–20 Hz) and were baseline corrected based on data from the 50 ms prestimulus interval. For each channel, we averaged the EEG epochs of all target and non-target stimuli to obtain ERP waveforms.

Hybrid P300 and rs-EEG. In this paper, patients whose CRS-R scores increased after 3 months of follow-up were recorded as "improved " patients, and patients whose CRS-R scores remained unchanged or decreased after 3 months were recorded as "non-improved". "Improved" patients are labeled as 1, and "non-improved" patients are labeled as

0. We collected P300 and rs-EEG signals from 22 patients separately. After preprocessing, the P300 and rs-EEG signals were combined 1:1 to form a hybrid P300 and rs-EEG signal. (the detailed process is shown in **Figure 2**) The feature information of patients with different prognosis conditions is found through feature extraction.

Prognosis prediction. We use four traditional machine learning algorithms: linear discriminant analysis (LDA) (Izenman, 2013), K-nearest neighbor (KNN) (Kramer & Kramer, 2013), support vector machine (SVM) (Pisner & Schnyer, 2020), Multi-Layer Perceptron (MLP) (Abdi, 1994) to make prognostic predictions on the processed data. Moreover, we use the proposed Self-Constructing Convolutional Neural Network (SCCNN, as shown in **Figure 2**) to predict and classify the extracted EEG signals. It mainly includes CNN layer, max pooling layer, BatchNormalization and Transformer. The multi-kernel convolution layer downsamples different frequency bands and extracts features. Transformer-based methods have achieved great success in many fields. The self-Attention mechanism is used to have the excellent ability to capture long-range dependencies. In SCCNN, the Adam optimizer with a weight decay rate of 0.0001 is used to minimize the loss, the batch size is 32, the learning rate is 0.00004, and Drop_out is set to 0.3.

Besides, We quantify our experimental outcomes utilizing the Area Under the Receiver Operating Characteristic Curve (AUC, Calculated using Python's sklearn.metrics.roc_auc_score function.) and Accuracy (ACC) :

$$ACC = \frac{TP+TN}{TP+TN+TP+FN} \tag{1}$$

where True Positive (TP) is the number of "positive" (i.e., improved patients) result retrieved by the classifier; True Negative (TN) is the number of "negative" (i.e., non-improved patient) result not retrieved by the classifier; False Positives (FP) are the classifier that incorrectly retrieved the number of "negative" results found; False Negatives (FN) are the number of "positive" results not retrieved by the classifier.

Results

In this section, we detail the experiments conducted and the results obtained using our proposed method. We employed our SCCNN model alongside four machine learning algorithms for validation purposes.

During the experiments, we combined P300 with rs-EEG signals from 22 patients across various paradigms. We extracted different frequency band features from the rs-EEG, which were then integrated with the P300. Subsequently, we applied 4 machine learning techniques to predict patient outcomes. The outcomes of these predictions are depicted in **Table 2** and illustrated in **Figure 3**.

As depicted in **Table 2**, the accuracy of the combined P300 and rs-EEG data across each frequency band for predicting the prognosis of patients with DoC consistently exceeds 75%. Utilizing the SCCNN has further enhanced the accuracy of cross-subject prognostic predictions, thereby validating the efficacy of our proposed method for this task.

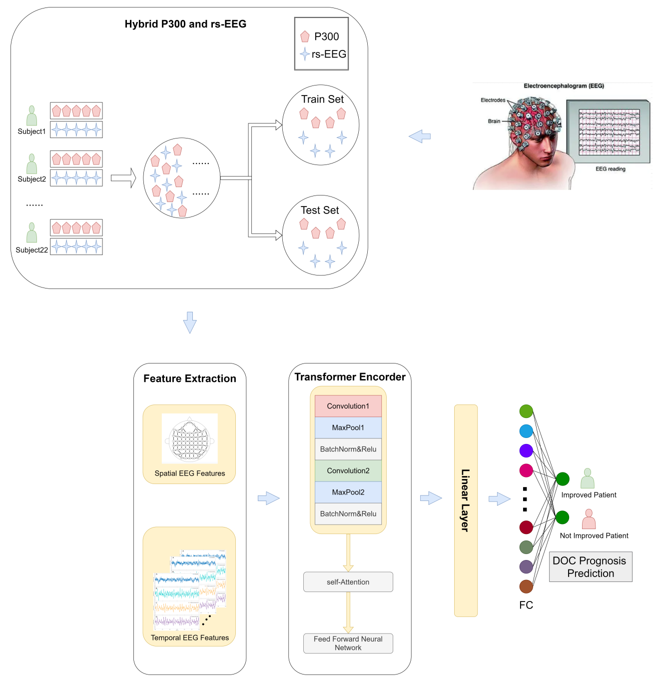

Figure 2: The overall structure of SCCNN.

Interestingly, when conducting cross-subject predictions using only the rs-EEG data from individual frequency bands, the delta band outperformed the others. The inclusion of the P300 signal resulted in improvements across the board, with the combined P300+delta signal exhibiting enhancements, albeit not as pronounced as those observed in other frequency bands. This observation opens up a new avenue for future research. Notably, the P300+alpha combination yielded the most favorable outcomes, indicating a strong correlation between the alpha band and patient prognosis.According to the mesocircuit hypothesis (Schiff, 2010), normal alpha activity is generated in the thalamus and reflects the intact functioning of thalamo-cortical loops, which are a prerequisite for consciousness (Schiff, 2010; Roux et al., 2013; Sokoliuk & Cruse, 2018). When these loops are structurally or functionally disrupted, consciousness is reduced or absent (Schiff, 2010). The presence of alpha activity indicates intact thalamocortical connections, such that future recovery of consciousness is a possibility. This is also consistent with our experimental results.

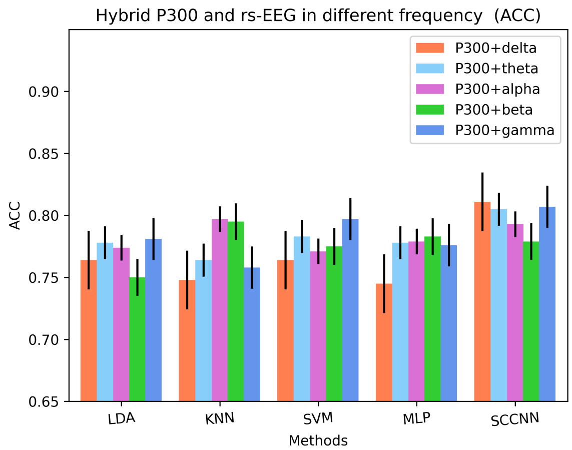

Figure 3: Cross-subject prognosis prediction results of hybrid P300 and rs-EEG signals in different frequency bands.

Table 2: Predicting prognosis of patients with DoC using hybrid P300 and rs-EEG.

Feature	Method	ACC	AUC
P300+delta	LDA	0.764	0.741
	KNN	0.748	0.728
	SVM	0.764	0.735
	MLP	0.745	0.729
	SCCNN	**0.811**	**0.803**
P300+theta	LDA	0.778	0.754
	KNN	0.764	0.745
	SVM	0.783	0.760
	MLP	0.778	0.773
	SCCNN	**0.805**	**0.762**
P300+alpha	LDA	0.774	0.748
	KNN	0.797	0.793
	SVM	0.771	0.743
	MLP	0.779	0.766
	SCCNN	**0.793**	**0.763**
P300+beta	LDA	0.750	0.728
	KNN	0.795	0.797
	SVM	0.775	0.747
	MLP	0.783	0.757
	SCCNN	**0.779**	**0.764**
P300+gamma	LDA	0.781	0.755
	KNN	0.758	0.752
	SVM	0.797	0.771
	MLP	0.776	0.753
	SCCNN	**0.807**	**0.810**

Discussion

Rs-EEG has been shown to provide diagnostic and prognostic information for patients with different brain diseases. Dukic et al. (Dukic et al., 2022) found that rs-EEG can reliably and quantitatively capture abnormal patterns of motor and cognitive network disruption in amyotrophic lateral sclerosis. Their data demonstrate that novel phenotyping using neuroelectric signal analysis can distinguish disease subtypes based exclusively on different patterns of network disturbances. Saes et al. (Saes et al., 2021) investigated whether rs-EEG parameters recorded early after stroke could predict Fugl-Meyer motor score (FM-UE) six months later. They demonstrated for the first time that rs-EEG parameters can also serve as prognostic biomarkers of stroke recovery. Schorr et al. (Schorr et al., 2016) investigated differences of EEG coherence within (short-range), and between (long-range) specified brain areas as diagnostic markers for different states of DoC and their predictive value for recovery from UWS. These findings suggest that rs-EEG consistency can be a predictor of recovery from UWS and has a diagnostic value.

Similarly, P300 has been repeatedly proven to be useful in detecting the level of consciousness of patients with DoC. For example, P300 has been confirmed to be different among subjects with different prognosis, which was also confirmed in previous study (Li et al., 2022). That is, there was a significant difference in P300 between patients with different prognosis. Pan et al. (Pan, Liang, et al., 2023) proposed a novel spatio-temporal self-constructing graph neural network (ST-SCGNN) for cross-subject emotion recognition and consciousness detection. Wang et al. (Wang et al., 2023) proposed a domain adaptation-based decoding algorithm called WD-ADSTCN to improve P300 signal detection in DoC patients. The experimental results showed that the proposed method can be applied to the P300 BCI system in DoC patients, which has important implications for the clinical diagnosis and prognosis of these patients.

Here, we conducted ablation experiments to compare the impact of different modules on prognosis prediction accuracy. As shown in **Table 3**, after adding Batch Normalization, the accuracy of all frequency bands increased by more than 7%, with an average increase of 9.2%. In addition, we borrowed from the popular CNN + Transformer mechanism in the image field and used it in our cross-subject and cross-paradigm prediction of the prognosis of patients with consciousness disorders. By superimposing the attention network and the fully connected layer, we obtained optimized feature vectors. This vector pays attention to the connection between patients and the direct correlation between each part of the sequence and the partial results that have been output, so that the neural network can better extract effective features of patients with different prognosis, thereby achieving higher prediction accuracy. After adding Transformer, the accuracy of all frequency bands has improved, with an average increase of 3.1%.

Moreover, we conducted ablation experiment on multimodal signals to verify the effectiveness of our fusion method. As shown in **Figure 4**, using hybrid P300 and rs-EEG, the improvement is relatively large. Under the machine learning method, the combined signal improved by 26.5% and 27.6% respectively compared with using P300 and rs-EEG alone. When using SCCNN, the combined signal is improved by 20.3% and 21.6% compared to using P300 and rs-EEG alone. It indicated that hybrid P300 and rs-EEG can effectively predict the prognosis of patients. In addition, we did a t-test on the accuracy of the three modalities, with a P-value <0.05. Moreover, the distribution of the probability density function was plotted (as shown in **Figure 5(a)(b)**), and it can be seen that the enhancement brought by the hybrid signals is significant compared with one signal alone. The experimental results demonstrated that hybrid P300 and rs-EEG can effectively improve the accuracy of predicting the prognosis of patients with DoC.

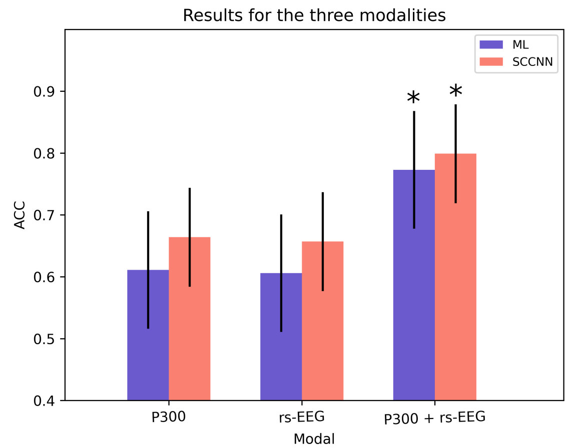

Figure 4: Prediction accuracies of three signals under machine learning and SCCNN. t-test: * $p < 0.05$.

Table 3: Ablation study on SCCNN. Improvement reports after new modules are added.

Feature	Method	ACC	Improve(ACC)	AUC
P300+delta	CNN	0.718	-	0.668
	CNN+BN	0.778	+8.4%	0.799
	SCCNN	**0.811**	**+13.0%**	**0.803**
P300+theta	CNN	0.714	-	0.684
	CNN+BN	0.780	+9.3%	0.791
	SCCNN	**0.805**	**+12.7%**	**0.762**
P300+alpha	CNN	0.718	-	0.796
	CNN+BN	0.780	+8.6%	0.812
	SCCNN	**0.793**	**+10.4%**	**0.763**
P300+beta	CNN	0.711	-	0.673
	CNN+BN	0.765	+7.6%	0.819
	SCCNN	**0.779**	**+9.6%**	**0.764**
P300+gamma	CNN	0.691	-	0.701
	CNN+BN	0.774	+12.0%	0.826
	SCCNN	**0.807**	**+16.8%**	**0.810**

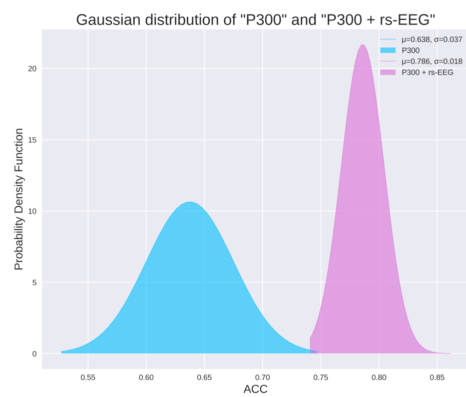

(a)

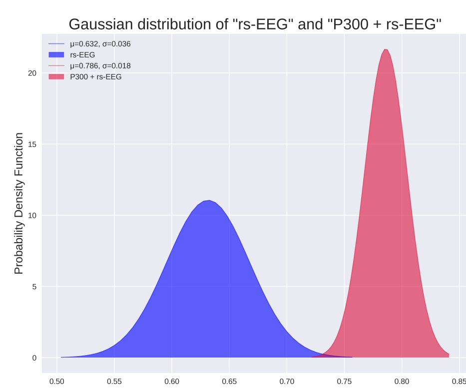

(b)

Figure 5: Comparison of probability density functions of single and hybrid signals.

In this study, we successfully integrated two distinct types of neurological signals for the first time, utilizing a composite of P300 and rs-EEG to predict patient outcomes across different paradigms and subjects. Our experimental results were promising. Ablation studies demonstrated that the combination of these signals significantly enhances predictive accuracy. This finding underscores the importance of the P300+rs-EEG fusion in prognostication for patients with DoC. The hybrid signal may be considered a potential biomarker and serve as a critical reference in the prognostic evaluation of DoC patients. Furthermore, our research supports the clinical application of P300+rs-EEG fusion in forecasting patient outcomes.

Acknowledgments

This work was supported by the STI 2030-Major Projects under grant 2022ZD0208900, Guangdong Basic and Applied Basic Research Foundation under grant 2023A1515140100.

References

Abdi, H. (1994). A neural network primer. *Journal of Biological Systems*, *2*(03), 247–281.

Bai, Y., Lin, Y., & Ziemann, U. (2021). Managing disorders of consciousness: the role of electroencephalography. *Journal of Neurology*, *268*, 4033–4065.

Bai, Y., Xia, X., & Li, X. (2017). A review of resting-state electroencephalography analysis in disorders of consciousness. *Frontiers in neurology*, *8*, 471.

Dukic, S., McMackin, R., Costello, E., Metzger, M., Buxo, T., Fasano, A., … others (2022). Resting-state EEG reveals four subphenotypes of amyotrophic lateral sclerosis. *Brain*, *145*(2), 621–631.

Fernández-Espejo, D., & Owen, A. M. (2013). Detecting awareness after severe brain injury. *Nature Reviews Neuroscience*, *14*(11), 801–809.

Gantner, I. S., Bodart, O., Laureys, S., & Demertzi, A. (2013). Our rapidly changing understanding of acute and chronic disorders of consciousness: challenges for neurologists. *Future Neurology*, *8*(1), 43–54.

Giacino, J. T., Ashwal, S., Childs, N., Cranford, R., Jennett, B., Katz, D. I., … others (2002). The minimally conscious state: definition and diagnostic criteria. *Neurology*, *58*(3), 349–353.

Giacino, J. T., Fins, J. J., Laureys, S., & Schiff, N. D. (2014). Disorders of consciousness after acquired brain injury: the state of the science. *Nature Reviews Neurology*, *10*(2), 99–114.

Izenman, A. J. (2013). Linear discriminant analysis. In *Modern multivariate statistical techniques: regression, classification, and manifold learning* (pp. 237–280). Springer.

Jennett, B., & Plum, F. (1972). Persistent vegetative state after brain damage: a syndrome in search of a name. *The Lancet*, *299*(7753), 734–737.

Johnson, L. S. M., & Lazaridis, C. (2018). The sources of uncertainty in disorders of consciousness. *AJOB neuroscience*, *9*(2), 76–82.

Kramer, O., & Kramer, O. (2013). K-nearest neighbors. *Dimensionality reduction with unsupervised nearest neighbors*, 13–23.

Laureys, S., Celesia, G. G., Cohadon, F., Lavrijsen, J., León-Carrión, J., Sannita, W. G., … others (2010). Unresponsive wakefulness syndrome: a new name for the vegetative state or apallic syndrome. *BMC medicine*, *8*, 1–4.

Li, J., Huang, B., Wang, F., Xie, Q., Xu, C., Huang, H., & Pan, J. (2022). A Potential Prognosis Indicator Based on P300 Brain–Computer Interface for Patients with Disorder of Consciousness. *Brain Sciences*, *12*(11), 1556.

Luauté, J., Morlet, D., & Mattout, J. (2015). BCI in patients with disorders of consciousness: clinical perspectives. *Annals of Physical and Rehabilitation Medicine*, *58*(1), 29–34.

Monti, M. M., Laureys, S., & Owen, A. M. (2010). The vegetative state. *Bmj*, *341*.

Pan, J., Liang, R., He, Z., Li, J., Liang, Y., Zhou, X., … Li, Y. (2023). St-scgnn: A spatio-temporal self-constructing graph neural network for cross-subject eeg-based emotion recognition and consciousness detection. *IEEE Journal of Biomedical and Health Informatics*, 1-12. doi: 10.1109/JBHI.2023.3335854

Pan, J., Wang, L., Huang, H., Xiao, J., Wang, F., Liang, Q., … Xie, Q. (2023). A hybrid brain–computer interface combining p300 potentials and emotion patterns for detecting awareness in patients with disorders of consciousness. *IEEE Transactions on Cognitive and Developmental Systems*, *15*(3), 1386-1395. doi: 10.1109/TCDS.2022.3213194

Pan, J., Xie, Q., Qin, P., Chen, Y., He, Y., Huang, H., … others (2020). Prognosis for patients with cognitive motor dissociation identified by brain-computer interface. *Brain*, *143*(4), 1177–1189.

Pisner, D. A., & Schnyer, D. M. (2020). Support vector machine. In *Machine learning* (pp. 101–121). Elsevier.

Rossi Sebastiano, D., Varotto, G., Sattin, D., & Franceschetti, S. (2021). EEG assessment in patients with disorders of consciousness: aims, advantages, limits, and pitfalls. *Frontiers in Neurology*, *12*, 649849.

Roux, F., Wibral, M., Singer, W., Aru, J., & Uhlhaas, P. J. (2013). The phase of thalamic alpha activity modulates cortical gamma-band activity: evidence from resting-state MEG recordings. *Journal of Neuroscience*, *33*(45), 17827–17835.

Saes, M., Meskers, C. G., Daffertshofer, A., van Wegen, E. E., Kwakkel, G., et al. (2021). Are early measured resting-state EEG parameters predictive for upper limb motor impairment six months poststroke? *Clinical Neurophysiology*, *132*(1), 56–62.

Schiff, N. D. (2010). Recovery of consciousness after brain injury: a mesocircuit hypothesis. *Trends in neurosciences*, *33*(1), 1–9.

Schorr, B., Schlee, W., Arndt, M., & Bender, A. (2016). Coherence in resting-state EEG as a predictor for the recovery from unresponsive wakefulness syndrome. *Journal of neurology*, *263*, 937–953.

Sitt, J. D., King, J.-R., El Karoui, I., Rohaut, B., Faugeras, F., Gramfort, A., … Naccache, L. (2014). Large scale screening of neural signatures of consciousness in patients in a vegetative or minimally conscious state. *Brain*, *137*(8), 2258–2270.

Sokoliuk, R., & Cruse, D. (2018). Listening for the rhythm of a conscious brain. *Brain*, *141*(11), 3095–3097.

Stam, C. J., Montez, T., Jones, B., Rombouts, S., Van Der Made, Y., Pijnenburg, Y. A., & Scheltens, P. (2005).

Disturbed fluctuations of resting state EEG synchronization in Alzheimer's disease. *Clinical neurophysiology*, *116*(3), 708–715.

Wang, F., Wan, Y., Li, Z., Qi, F., & Li, J. (2023). A cross-subject decoding algorithm for patients with disorder of consciousness based on P300 brain computer interface. *Frontiers in Neuroscience*, *17*.